

# Domain wall trapping in controlled submicron ferromagnetic elements

A. Hirohata, Y. B. Xu, C. C. Yao, H. T. Leung, W. Y. Lee, S. M. Gardiner, D. G. Hasko, and J. A. C. Bland<sup>a)</sup>

*Cavendish Laboratory, University of Cambridge, Madingley Road, Cambridge CB3 0HE, England*

S. N. Holmes

*Cambridge Research Laboratory, Toshiba Research Europe Limited, 260 Cambridge Science Park, Milton Road, Cambridge CB4 0WE, England*

The domain configuration in permalloy wires (30 nm thick, 10  $\mu\text{m}$  wide, and 205  $\mu\text{m}$  long) with a wide size range of a narrow central bridge (5  $\mu\text{m}$  long and  $w$   $\mu\text{m}$  wide;  $0.5 \leq w \leq 10$   $\mu\text{m}$ ) were investigated in both their demagnetized and remanent states using magnetic force microscopy and the results were confirmed by micromagnetic calculations. At the bridge region, domain walls were found to be shifted by a small external field. Scanning magneto-optical Kerr effect revealed that the coercivity in these structures are the same as that in a straight wire, suggesting that domain wall movement is the dominant process in the magnetization reversal of these structures. © 2000 American Institute of Physics. [S0021-8979(00)35408-1]

## I. INTRODUCTION

A great deal of attention has been paid to the resistivity associated with the electron scattering at magnetic domain walls.<sup>1-5</sup> Recent progress in nanofabrication techniques enables researchers to identify the domain wall scattering contribution from the magnetoresistance (MR) data.<sup>1-3</sup> Discontinuous changes of the MR were observed in Ni wires caused by the nucleation and movement of domain walls.<sup>1</sup> A negative domain wall contribution to the MR was also found in micron-size Fe wires forming multistripe domains.<sup>2</sup> NiFe cross-shape wires have been observed to limit the number of domain walls at the junction area, which also show a negative contribution to the MR.<sup>3</sup> Theoretical interpretations were proposed recently using weak localization<sup>4</sup> and spin-flip scattering.<sup>5</sup> Mesoscopic junction structures offer an attractive alternative route for localizing domain walls for such MR studies. However, as a first step, the precise domain structure needs to be clarified.

In this study, we investigated ferromagnetic thin film junctions structured into a range of geometries which act to trap domain walls in the vicinity of the bridge in which the MR behavior can be investigated. Scanning probe microscopy (SPM, Digital Instruments, Nanoscope III) was used to reveal the role of both the size and shape of the structures in the formation of domain walls, and this was supported by micromagnetic calculations. Scanning magneto-optical Kerr effect (SMOKE) measurements of the local  $M-H$  loop were also carried out.

## II. EXPERIMENTAL PROCEDURE

A 3 nm Au/30 nm Ni<sub>80</sub>Fe<sub>20</sub> continuous film structure was deposited on a GaAs (100) substrate in ultrahigh vacuum (UHV). The permalloy layers were deposited at a rate of 0.25 nm/min. The pressure during the growth was

$5.0 \times 10^{-9}$  Torr, while the substrate was held at 300 K. The permalloy wires (30 nm thick, 1–50  $\mu\text{m}$  wide, and 205  $\mu\text{m}$  long) with a narrow central bridge of width  $w$  section which behaves as a domain wall trapping junction (5  $\mu\text{m}$  long and  $w = 0.5, 1, 2, 5,$  and  $10$   $\mu\text{m}$  wide bridge and 10  $\mu\text{m}$  long “bowtie”) were fabricated by electron beam lithography and optimized pattern transfer techniques based on a combination of both dry and wet etching. Typical examples of the structures are shown in Fig. 1.

The permalloy structures were observed in both their demagnetized and remanent states by magnetic force microscopy (MFM) together with atomic force microscopy (AFM). A commercial Si probe (Digital Instruments, Pointprobe magnetic force sensor MESP) coated with CoCr was used and the distance between probe and sample was set as 5 nm for the AFM tapping mode and 100 nm for MFM measurements.<sup>6</sup> The tip of this probe was magnetized before each observation. The magnetic probe typically has a spring constant of 2.8 N/m and a resonance frequency of 75 kHz. The resolving power of these two forms of microscopy was approximately 10 nm for AFM and 100 nm for MFM, respectively. The local coercivity was also measured by SMOKE in order to understand the magnetization reversal process in the junctions.

## III. RESULTS AND DISCUSSION

Figure 2 shows MFM images of the 10  $\mu\text{m}$  wide permalloy wires with a narrow central bridge [5  $\mu\text{m}$  long and  $w =$  (a) 0.5, (b) 1, (c) 2, and (d) 5  $\mu\text{m}$  wide bridge] in the demagnetized state. Single domains are seen in the bridge regions in the range of  $0.5 \leq w \leq 2$   $\mu\text{m}$ . It should be noted that in the bridge, domain walls are trapped at the both ends; one wall (A) is rounded and ends at the junction of the bridge and the wire [see left-hand side junction area in Figs. 2(a)–2(c)], while another wall (B) is penetrating into the bridge as a straight wall and is connected to the other walls starting from the corners of the wire region [see right-hand side in Figs. 2(a)–2(c)]. In addition, one wall (C), which

<sup>a)</sup> Author to whom correspondence should be addressed; electronic mail: jacb1@phy.cam.ac.uk

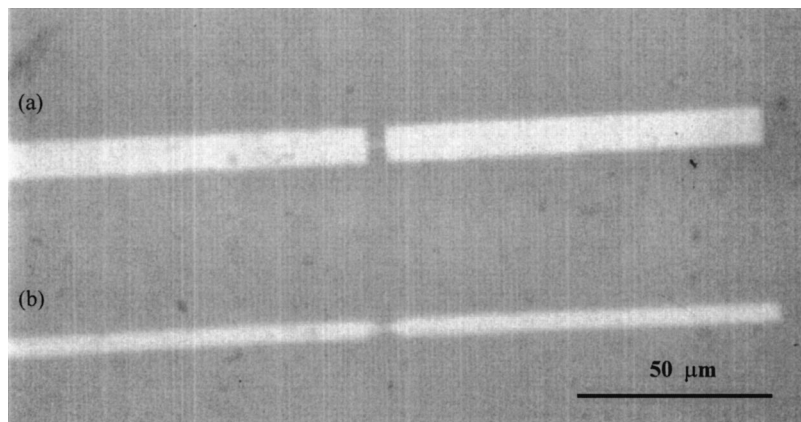


FIG. 1. Optical micrograph of the permalloy wires (a) 30 nm thick, 10  $\mu\text{m}$  wide, and 205  $\mu\text{m}$  long with a narrow central bridge of width  $w$  section which behaves as a domain wall trapping junction (5  $\mu\text{m}$  long and  $w = 0.5 \mu\text{m}$  wide) and (b) 30 nm thick, 5  $\mu\text{m}$  wide, and 205  $\mu\text{m}$  long with 10  $\mu\text{m}$  long "bowtie."

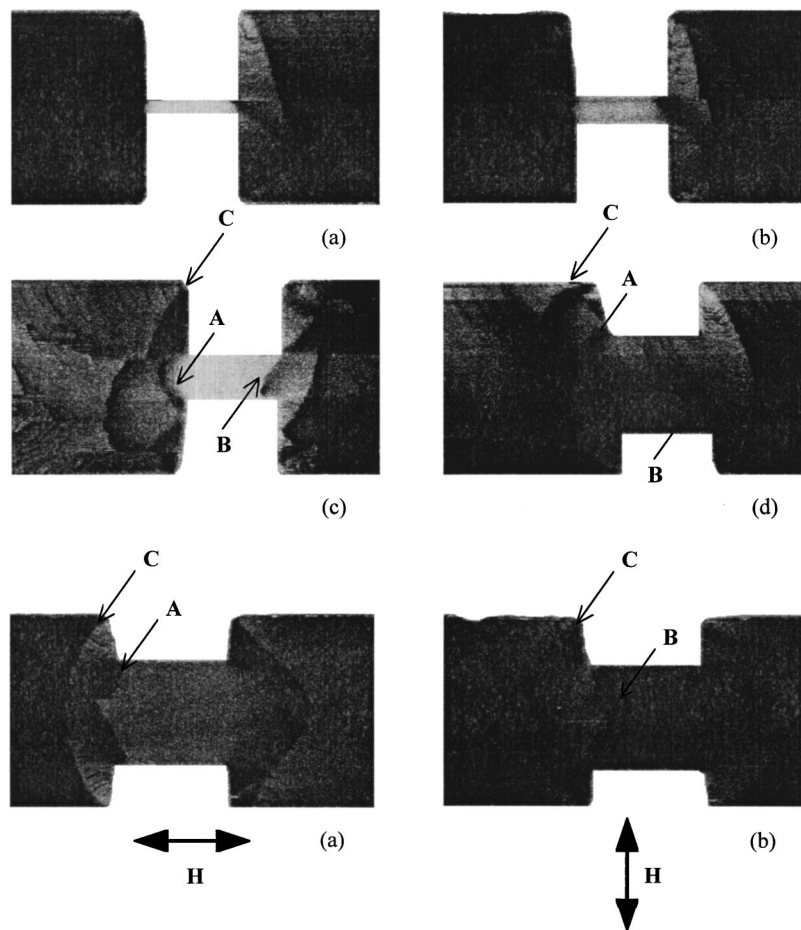


FIG. 2. MFM images of the permalloy wires (30 nm thick, 10  $\mu\text{m}$  wide, and 205  $\mu\text{m}$  long) with a narrow central bridge of width  $w$  section which behaves as a domain wall trapping junction (5  $\mu\text{m}$  long and  $w =$  (a) 0.5, (b) 1, (c) 2, and (d) 5  $\mu\text{m}$  wide) in the demagnetized state.

FIG. 3. MFM images of the permalloy wires (30 nm thick, 10  $\mu\text{m}$  wide, and 205  $\mu\text{m}$  long) with a narrow central bridge (5  $\mu\text{m}$  long and  $w = 5 \mu\text{m}$  wide) in the remanent state. The direction of the applied magnetic field is indicated below.

connects both corners of the end of the wire region, is observed as shown on the left-hand side wire in Fig. 2. With the increase of  $w$ , the latter wall B penetrates into the bridge and stays in the middle, while another wall A shifts slightly in the same direction and the wall C stays at the same position [see Fig. 2(d)].

The bridge structures were also observed in the remanent state and wall movements were seen only with  $w = 5 \mu\text{m}$  as shown in Fig. 3. This suggests that the domain walls observed in the other samples ( $w \leq 2 \mu\text{m}$ ) are very stable and good candidates for the domain wall resistivity measurements. On the other hand, in the case of  $w = 5 \mu\text{m}$ , in the remanent state after the application of an external magnetic field (1 T) along the wire [see Fig. 3(a)], the wall A stays at the same position as seen in the demagnetized state, while

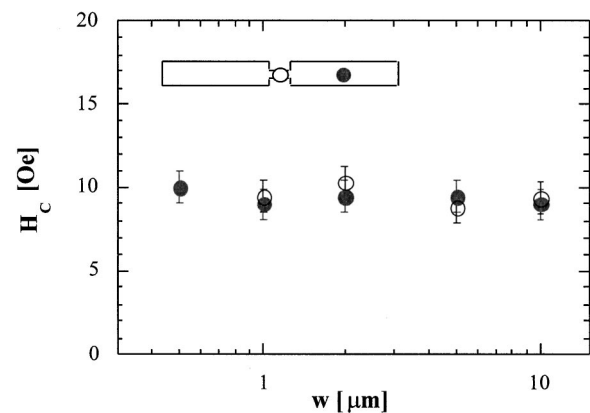


FIG. 4. Coercive force of the permalloy bridge structures. Open circles indicate the local coercivity at the bridges, while closed ones show that in the middle of the wire regions.

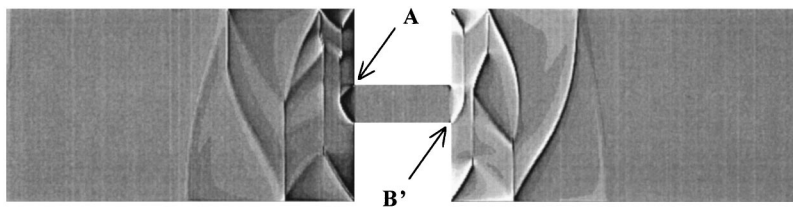


FIG. 5. Micromagnetic simulations for the bridge region of the permalloy wires (30 nm thick, 10  $\mu\text{m}$  wide, and 205  $\mu\text{m}$  long) with a narrow central bridge (5  $\mu\text{m}$  long and  $w=2$   $\mu\text{m}$  wide) in the demagnetized state.

the wall B in the middle of the bridge is likely to shift in the same direction and joined together with the wall A at the end of the bridge, suggesting that the domain wall B is unstable and plays an important role of the domain wall movement during the magnetization reversal process. In the remanent states following the application of a perpendicular field, wall B is not shifted and wall A disappears as shown in Fig. 3(b). The results above mean that the walls A and B are easily moved by the applied field and wall A becomes wall C. These results suggests that the bridge with  $w=5$   $\mu\text{m}$  is likely to be relevant for the wall velocity measurements within the bridge under a small applied field.

Figure 4 shows the coercivity of the bridge structures. It should be noted that the variation of the coercivity with the width of the bridge is very small and has almost the same value as that of the straight wire ( $w=10$   $\mu\text{m}$ ), suggesting that the domain nucleation from the edge of the wire regions is dominant in the magnetization reversal process. This is consistent with the magnetic domain wall movement observed by MFM.

#### IV. NUMERICAL CALCULATIONS

Micromagnetic numerical calculations were carried out to confirm the domain wall configurations of the bridge structures using a finite difference method.<sup>7</sup> The system was divided into 30 nm cubic cells. The demagnetizing field, magnetic anisotropy field and the exchange field were calculated at the position of each cell which was assumed to possess a constant magnitude of magnetization  $M_s$ . The magnetization can point in any direction.  $M_s$  was randomly aligned at first and each cell magnetization rotated in a direction so as to reduce the total energy at the cell position. The total energy of the samples was also calculated and the stable domain configuration was defined at the minimum energy.

The results of numerical simulations of the  $w=2$   $\mu\text{m}$  bridge structure is shown in Fig. 5. In this picture, the magnitude of the divergence of the magnetization is shown by the gray scale, which indicates the same contrast as that in the MFM images. Since the magnetization in the domain walls is rapidly rotating, the walls are shown as a combination of black and white lines, corresponding to a high divergence value. Figure 5 shows almost the same magnetic domain configuration as that observed by MFM. The domain

wall A in Fig. 5 is the same as the wall A seen in Fig. 2(c). However, the position of the wall B' in Fig. 5 is different from the wall B in Fig. 2(c), suggesting that the wall B is affected by the local magnetic field caused by the MFM tip and shifted into the bridge region. This also supports the experimental observation that domain wall movement is the dominant process in the magnetization reversal process in these structures.

#### V. CONCLUSIONS

We investigated the domain configurations in permalloy wires (30 nm thick, 10  $\mu\text{m}$  wide, and 205  $\mu\text{m}$  long) with a wide size range of a narrow central bridge (5  $\mu\text{m}$  long and  $w$   $\mu\text{m}$  wide;  $0.5 \leq w \leq 10$   $\mu\text{m}$ ) prepared on a GaAs (100) substrate in both their demagnetized and remanent states using MFM. Domain walls are observed at the bridge region and are easily moved by an external field. SMOKE results show that the variation of the coercivity with the bridge width  $w$  is very small, suggesting that domain wall movement is the dominant process in the magnetization reversal of these structures. The observed domain configurations are supported by the results of micromagnetic simulations. These structures especially with narrow bridges suggest a possible way of detecting the domain wall resistivity in a low magnetic field, while providing insight into the domain wall reversal process in flat wire structures.

#### ACKNOWLEDGMENTS

The authors gratefully acknowledge the financial support of the EPSRC and the EU (SUBMAGDEV and MASSDOTS). A.H. would like to thank Toshiba Europe Research Limited, Cambridge Overseas Trust and Selwyn College (Cambridge) for their financial support.

<sup>1</sup>K. Hong and N. Giordano, Phys. Rev. B **51**, 9855 (1995); Europhys. Lett. **36**, 147 (1996).

<sup>2</sup>U. Ruediger, J. Yu, S. Zhang, A. D. Kent, and S. S. P. Parkin, Phys. Rev. Lett. **80**, 5639 (1998).

<sup>3</sup>Y. B. Xu, C. A. F. Vaz, A. Hirohata, C. C. Yao, W. Y. Lee, J. A. C. Bland, F. Rousseaux, E. Cambriil, and H. Launois, J. Appl. Phys. **85**, 6178 (1999).

<sup>4</sup>G. Tataru and H. Fukuyama, Phys. Rev. Lett. **78**, 3773 (1997).

<sup>5</sup>P. M. Levy and S. Zhang, Phys. Rev. Lett. **79**, 5110 (1997).

<sup>6</sup>K. L. Babcock, V. B. Elings, J. Shi, D. D. Awschalom, and M. Dugas, Appl. Phys. Lett. **69**, 705 (1996).

<sup>7</sup>H. T. Leung, A. Hirohata, W. Y. Lee, and J. A. C. Bland (unpublished).